Proceedings of ICNMM2006
Fourth International Conference on Nanochannels, Microchannels and Minichannels
June 19-21, 2006, Limerick, Ireland

ICNMM2006-96118

MASS FLOW RATE MEASUREMENTS IN NITROGEN FLOWS

Pierre Perrier
Timothée Ewart
Université de Provence
Ecole Polytechnique Universitaire de Marseille
Département de Mécanique Energétique
UMR CNRS 6595
5 rue E.Fermi, 13453 Marseille, France
Email: pierre.perrier@polytech.univ-mrs.fr
Email: timothee.ewart@polytech.univ-mrs.fr

J. Gilbert Méolans*
Irina A. Graur
Université de Provence
Ecole Polytechnique Universitaire de Marseille
Département de Mécanique Energétique
UMR CNRS 6595
5 rue E.Fermi, 13453 Marseille, France
Email: gilbert.meolans@polytech.univ-mrs.fr
Email: irina.graour@polytech.univ-mrs.fr

ABSTRACT

The main objective of this experimental investigation on the gas flow slip regime is to measure the mass flow rate in isothermal steady flows through cylindrical micro tubes. Two technical procedures devoted to mass flow rate measurements are compared, and the measured values are also compared with the results yielded by different approximated analytical solution of the gas dynamics continuum equations. Satisfactory results are obtained and the way is clearly open to measuring mass flow rates for higher Knudsen numbers, over all the micro flow transitional regime.

NOMENCLATURE

k_λ coefficient depending on the molecular interaction model
m mass of the gas in the outlet tank
s standard deviation
u streamwise velocity
D diameter of the tube
Kn Knudsen number
L length of the tube
P pressure
Q_m mass flow rate
$\mathcal{P}$ ratio P_{in}/P_{out}
$\mathcal{R}$ specific gas constant
T temperature
V outlet tank volume
α tangential momentum accommodation coefficient
τ experiment time length
λ mean free path
μ viscosity
σ_p first order velocity slip coefficients
σ_{2p} second order velocity slip coefficients

Subscripts

s Slip parameter
out outlet tank
in inlet tank
m mean parameter
ref reference value
exp experimental value

INTRODUCTION

Since the early eighties, mass flow rates in microchannels have mostly been measured using a liquid drop method [1] – [6]. So far, in order to determine volumes variations and mass flow rates, the drop movement has been either observed through a low power microscope [1] or determined visually as a meniscus of water travelling along the marked scale of a syringe [3]

*Address all correspondence to this author.

or detected by means of optoelectronic sensors [6]. Other authors [7], [8] have used a different method involving a sensitive dual-tank accumulation technique based on the measurements of the pressure differences between an accumulation reservoir and a reference tank.

Another approach used by some authors involves the utilization of flowmeters [9] or high precision flow sensors [10] to measure the mass flow rate. But this kind of measurement is restricted to relatively high mass flow rates about $10^{-8} kg/s$.

The main aim of the present study focusing on the gas flow regime is the validation of a mass flow rate measurement method based on direct pressure change measurements. Two methods are presented:

1. The liquid drop method already used and tested in previous years, developed here using new equipment.

2. A new method (new as far as the measurement range is concerned) based on constant volume pressure measurements, using up-to-date Inficon™ pressure gauges with a resolution of 1.9, 0.19 and 0.019 *Pa*.

Let us point out that the experimental methods mentioned at the beginning of the introduction generally concern experiments carried out in channels with rectangular (or trapezoidal) cross-sections, while the present measurements have been carried out in microtubes. Experiments in this type of geometry are rare [11] – [13]: they have been made in tubes of relatively large diameter ($3.64 cm$ in [11]), or using capillary packets of 10 to 640 capillaries [12], which makes difficult the control the diameter of the capillaries.

Then the different features and the respective characteristics of the two experimental techniques are compared. Their respective results are analyzed and compared with theoretical results derived from continuum approaches taking into account the rarefaction effects present in microflows.

Although the NS equations are derived from a first order kinetic solution, many authors [6], [14] – [17] have suggested, using in this framework the velocity slip conditions of second order according to the Knudsen number, to better take into account the rarefied effects for the moderately rarefied gas flows. The implementation of these conditions leads to an additional term in the mass flow rate expression, proportional to the second order in Knudsen number.

The presence of the high order terms in the mass flow expression has also been highlighted by other authors [18]: by applying the BGK model in the Boltzmann equation for the cylindrical Poiseuille flow and in the case of diffuse scattering, the asymptotic formula for the flow rate containing the terms of second and also third order in Knudsen number was obtained [18].

The analysis of the present mass flow rate measurements reveals the existence of so-called "second order effects" for averaged Knudsen numbers larger than 0.1, as it was found in [4], [6]. Furthermore the velocity slip coefficients for the velocity slip condition of second order and the accommodation coefficient are deduced from experiments using various continuum approaches.

EXPERIMENTS

Description of the methodology and experimental set-up

Each of the experimental methods used in the present work to measure the mass flow rate through a micro tube involves the use of two constant volume tanks and so may be denoted "constant-volume technique". Both methods require very large tank volumes, much larger than the volumes of the micro tube and syringe in which the gas flows during the experiments (Fig. 1). Large tank sizes guarantee micro flow parameters independent from the time: although detectible (through their effects), the mass variations occurring in the tanks during the experiments do not call into question the steady assumption. Thus, we have to fix a range for the maximal suitable pressure variations in the second tank, according to the inlet and outlet conditions.

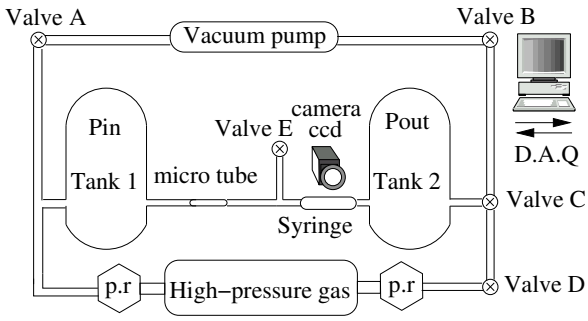

Figure 1. SCHEMATIC OF MASS FLOW EXPERIMENT.

The experimental set up shown in Fig. 1 takes into account these constraints. The gas flows through a fused silica micro tube fixed between two tanks in which the pressures remain very close to constant values P_{in} and P_{out}, respectively. A pressure regulator and a valve A (see Fig.1) are used to impose the pressure in the first tank. The pressure in the second tank is adjusted by means of another pressure regulator and three valves B, C and D (see Fig.1), to ensure better tightness. In this tank the pressure variation due to the gas flow through the micro tubes is fixed at $\pm 1\%$ of the tank pressure averaged over the duration of the experiment (for the experiment based on the pressure measurements). As a consequence, the relative pressure variation in the first tank remains close to $\pm 0.2\%$. This variation range means that the required experiment duration τ will vary from about five minutes for the highest mass flow rate measured ($10^{-9} kg/s$) to about fifty minutes for the lowest **(**$10^{-13} kg/s$**)**.

Table 1. DETECTOR STUDY RANGE, EVERY DETECTORS (A,B and C) ARE USED IN THEIR APPROPRIATE PRESSURE STUDY RANGE.

Detectors	A	B	C
Pressure limit max (Pa)	133322.	13332.2	1333.22
Pressure limit min (Pa)	13332.	1333.2	133.32

Table 2. Technical data for the gas detector. The three detectors have similar characteristics, but their full scales are different.

	Detectors (A,B and C)
Full scale FS (Pa)	133322. (A)
	13332.2 (B)
	1333.22 (C)
Accuracy	0.20 % of reading
Temperature effect on zero	0.0050 % FS / °K
Temperature effect on span	0.01 % of reading / °K
Resolution	0.0015 % FS

The pressure measurements were carried out using simultaneously two detectors chosen according to the pressure range (see Table 1). The first one (Inlet Detector) was located in the first tank, upstream from the micro tube while the second (Outlet Detector) was located downstream from the micro tube. The errors in pressure measurements in each tank depend on the characteristics of the pressure detectors, given in Table 2. Thus, in the pressure range observed during the experiments, the errors on the measurement of the outlet pressures were estimated smaller than 0.5%.

Moreover to obtain a significant and accurate pressure variation we also fixed a lower limit for the data acquisition, equal to 60 times the resolution. Thus the statistical processing involves a correct discrete distribution of a sufficient number of points.

It is also of great importance to measure the diameters of the tubes with a good accuracy because the analytical expression of the mass flow rate is proportional to the power four of the diameter. The surfaces of the inlet and outlet sections were scanned in environmental scanning mode (ESEM) with an electron microscope and the following estimation of the diameters may be retained:

$$D = 25.2 \pm 0.35\,\mu m. \tag{1}$$

For all the connections needed in the gas circuit, we used a standard vacuum material (Swagelock™ technology) to achieve the best tightness possible. The control of the tightness is all the more important as the pressures and mass flow rates to investigate are low. Leak estimations were provided by various tests. The leakage check was performed by pumping out the system (the pressure was fixed at the same low value in both tanks), and monitoring the pressure rise in the second (downstream) tank for several hours. The first step of the measurements was performed using detectors A and B. In that case, the lower pressure measured in the outlet tank was $\sim 1032Pa$. The leakage check was performed in these conditions. When the mean pressure was equal to $361.8Pa$ in both tanks and for a long experiment time (2 hours), the sensor did not detect any fluctuation of the signal: thus the pressure increase due to the leaks was lower than the sensor resolution ($0.19Pa$), which implies a leak rate smaller than $2.08 \cdot 10^{-14} kg/s$. For the mass flow range considered ($2 \cdot 10^{-12} - 2 \cdot 10^{-10} kg/s$) these results represent a satisfactory leak estimation: for the lowest mass flow rate measured, the error induced by the leaks is certainly much smaller than 1%.

Another experimental leakage check was carried out by means of helium detection (with a portable leak detector): the effect of the leaks on the mass flow rate was thus controlled as being smaller than $10^{-17} kg/s$. Therefore this effect was not taken into account when estimating the experimental errors.

The experiments were performed within a narrow temperature range around $296.5°K$, excluding any heat source in the environment. During each experiment, the temperature was not maintained but controlled to be sufficiently constant to justify the isothermal assumption. Thus, during each experiment the maximal instantaneous temperature deviation from its initial value was registered smaller than $0.5°K$, using temperature detector with $0.13°K$ accuracy. In the next Section, devoted to the measurement that was the most sensitive to the perturbing temperature variations, it will be shown that the non isothermal effects are negligible.

Utilizing the apparatus described in Fig. 1 and taking into account the previous methodological considerations, we used two different technical approaches for the measurements of mass flow rates through micro tubes: one consisting in registering the motion of a liquid drop in a calibrated pipette installed downstream from the micro tube (see Fig. 1), the other based on direct pressure rise measurements in the outlet tank. In the next paragraph this latter method is developed first for a clearer presentation.

Mass flow rate measurement 1 (pressure method)

Analysis of the non isothermal effects The first technique used to measure the mass flow rate consists in determining in the outlet tank a small pressure change due to the mass flowing from the micro tube. The disturbing temperature variation in the outlet tank could directly perturb the significance of the measurement. To make this clear, let us write for this tank

the law of perfect gases under the form:

$$P_{out}V = m\mathcal{R}T, \tag{2}$$

where V represents the outlet tank volume which remains constant during the experiment, $V = 65.71 \pm 1.5\ cm^3$, and $\mathcal{R}$ is the specific gas constant. P_{out}, T, m, are respectively, the pressure, temperature and mass of gas in the outlet tank, at any time t of the experiment time length τ. Let us define the variation dq of any thermodynamic parameter q, occurring in the tank during the experiment time length (whatever the reason of these variations). According to the previous section comments, these relative variations remain small, compared to 1. Therefore, they are obtained from (2), as verifying:

$$\frac{dP_{out}}{P_{out}} = \frac{dm}{m} + \frac{dT}{T}. \tag{3}$$

Dividing the two terms of equation (3) by the experimental time length τ and using equation (2) we obtain:

$$\frac{dm}{\tau} = \frac{V}{RT}\frac{dP_{out}}{\tau}(1-\varepsilon), \qquad \varepsilon = \frac{dT/T}{dP_{out}/P_{out}}. \tag{4}$$

If ε is very small compared to 1, disregarding the technical uncertainties, dm/τ may be identified to the mass flow rate Q_m flowing from the micro tube, and dP_{out} (termed below δP_{out}) will allow us direct measurement of Q_m. As pointed out in the previous paragraph, the maximal instantaneous temperature departure (from its initial value) registered during the experiments was smaller than half a degree. Such a departure certainly overestimates the probable temperature variation at any time. Therefore, from the various points (n is the number of points) acquired during the experimental time τ, we calculated the mean temperature value $\overline{T}$ and its corresponding standard deviation s, which appears here as a pertinent evaluation of the probable temperature variation. The sample standard deviation is defined by

$$s = \sqrt{\frac{1}{n-1}\sum_{i=1}^{n}(T_i - \overline{T})^2}, \tag{5}$$

where T_i is the registered data for the temperature. In the most unfavorable case this estimation leads to a relative variation $\delta T/T = s/T$ around the mean temperature equal to $2 \cdot 10^{-4}$, against $1 \cdot 10^{-2}$ for the relative variation $\delta P_{out}/P_{out}$: ε is clearly smaller than $2 \cdot 10^{-2}$. Thus the measurement based on the pressure rise may be considered as the measurement of an isothermal mass flow rate equal to

$$Q_m = \frac{V}{\mathcal{R}T}\frac{\delta P_{out}}{\tau}, \tag{6}$$

affected by a specific relative error equal to $\pm 2 \cdot 10^{-2}$ due to the temperature variation.

Pressure rise measurements Since the effects of the temperature variation are negligible, we may consider the flow through the micro tube as a steady flow between two tanks maintained at constant pressures P_{in} and P_{out} respectively. Moreover, the isothermal mass flow rate may be expressed in the form (6). To determine this mass flow rate we will use the registered data for the pressure P_i at the time instants t_i. The flow steady conditions physically justify the pressure rise interpolation by means of a linear fitting function of time

$$P_f(t) = at + b, \qquad a = \frac{\delta P_{out}}{\tau}. \tag{7}$$

Using the least-square method we handled a number of points n ranging between 1300 and 3800. The calculation of the coefficients a is characterized by a very convenient value of the usual determination coefficient r^2, greater than 0.9993. Under the reasonable assumption of negligible errors in determining the fixed time values t_i chosen, the calculation of the standard deviation for the coefficient a yields

$$\Delta a = \sqrt{\frac{n\sum_{i=1}^{n}(P_i - P_f(t_i))^2}{(n-2)\left(n\sum_{i=1}^{n}t_i^2 - \left(\sum_{i=1}^{n}t_i\right)^2\right)}}. \tag{8}$$

According to the previous remarks, formula (8) represents a correct estimation of the error on coefficient a (i.e. also on $\delta P_{out}/\tau$) and yields a relative error smaller than $\pm 0.1\%$. Thus, the usual evaluation of the measurement errors results from relations (6)-(8) as :

$$\frac{\Delta Q_m}{Q_m} = \frac{\Delta V}{V} + \frac{\Delta T}{T} + \frac{\Delta a}{a}, \tag{9}$$

where $\Delta T/T$ vanishes if the non-isothermal effects ($\pm 2\%$), $\Delta V/V$ is the uncertainty of the volume measure ($\pm 2\%$) and $\Delta a/a$ the error on coefficient a ($\pm 0.5\%$). Moreover, the leaks were estimated as totally negligible (see Section "Description of the methodology and experimental set-up"), we did not integrate them in the total uncertainty on the mass flow rate. Therefore, we obtain a full uncertainty on $\Delta Q_m/Q_m$ smaller than $\pm 4.5\%$.

Mass flow rate measurement 2 (drop method)

In the standard drop method, the mass flow rate is measured by determining the speed of a liquid drop moving in a calibrated

tube, using a low power microscope [1] or opto electronic sensors [6] or simply visually [3]. In the present work an oil drop was chosen because of its low saturation vapor ($1.33 \cdot 10^{-3} Pa$) to avoid a vaporizing effect on the moving surface of the drop. The drop was injected in the calibrated tube through the valve E (see Fig. 1) and its movement was recorded by means of a digital camera 1290×980 pixels. Thus the position of the drop was registered as a time function.

Since this drop method is known and was applied here only with new equipment we omit the detail description of the mass flow rate determination based on the drop movement and we list only the uncertainty on Q_m. Thus, considering the series of measurements investigated $\Delta Q_m/Q_m$ is close to $\pm 4.2\%$.

Background theory

For many years, pressure-driven slip flow within ducts or channels has received considerable attention. The many formulations of the analytical and semi-analytical solutions have been presented [16]. The analytical models derived from the Navier-Stokes equations or from other continuum equation systems require the use of the velocity slip boundary conditions. Several authors have recently proposed to use in this framework the velocity slip conditions of second-order according to the Knudsen number to better take into account the rarefied effects for the moderately rarefied gas flows. It should be noticed that the Navier-Stokes equations result from the first order Chapman-Enskog expansion and do not logically require the second order of boundary conditions, as for example the Burnett or QGD equations do. But, according to [14] if a certain degree of symmetry is present in the flow, the Burnett terms in the momentum equation are equal to zero far from the wall, so that second order slip can sometimes be meaningfully associated with the Navier-Stokes momentum equation.

The form of the second order velocity slip boundary condition when the streamwise velocity depends only on the direction normal to the wall and for a isothermal flow reads [14]:

$$u_s = \pm\sigma_p \frac{\mu}{P}\sqrt{2\mathcal{R}T}\left(\frac{\partial u}{\partial r}\right)_w - \\ -\sigma_{2p}\left(\frac{\mu}{P}\sqrt{2\mathcal{R}T}\right)^2\left(\frac{1}{r}\left(\frac{\partial}{\partial r}r\frac{\partial u}{\partial r}\right)\right)_w, \qquad (10)$$

where σ_p and σ_{2p} are the first and second order velocity slip coefficients, which depend on the reflection law. Therefore, the reflection process at the wall exerts a direct influence here, while the intermolecular forces act only through the viscosity coefficient, whatever the interaction model used in the gas. This appears in the expression of the mass flow rate and also in the pressure and velocity profiles [22]. It should be noted that equation (10) is written in terms of measurable quantities; for the application however, it is very convenient to characterize the rarefied flow as depending on the mean free path λ of the molecules or on the Knudsen number. The molecular mean free path is defined by the relation

$$\lambda = k_\lambda \frac{\mu}{P}\sqrt{2\mathcal{R}T}, \qquad (11)$$

where coefficient k_λ depends on the molecular interaction model. Very often, $k_\lambda = \sqrt{\pi}/2$ (i.e. a value close to that obtained from the hard sphere model (HS) [19]) is retained. Another possibility consists in using the expression deduced by Bird [20] for the variable hard sphere model (VHS), more general than the HS model. According to this model, coefficient k_λ is equal to $\frac{(7-2\omega)(5-2\omega)}{15\sqrt{\pi}}$, where ω, the viscosity index, depends on the type of gases (see Table 3). Within the VHS model the viscosity thermal dependence reads: $\mu = \mu_{ref}\left(\frac{T}{T_{ref}}\right)^\omega$. In this work, we used the VHS model. Using expression (11) for the mean free path, the velocity slip condition (10) may be rewritten as

$$u_s = \pm A_1 \lambda\left(\frac{\partial u}{\partial r}\right)_w - A_2\lambda^2\left(\frac{1}{r}\left(\frac{\partial}{\partial r}r\frac{\partial u}{\partial r}\right)\right)_w, \qquad (12)$$

where coefficients A_1 and A_2 may be presented in the form:

$$A_1 = \frac{\sigma_p}{k_\lambda}, \qquad A_2 = \frac{\sigma_{2p}}{k_\lambda^2}. \qquad (13)$$

Unlike the velocity slip coefficients, constants A_1 and A_2 depend on the interaction model used in the gas.

Many different theoretical values of coefficients A_1 and A_2 are proposed in the literature (see review articles [16], [21]). It can be seen that no agreement has yet been reached on the correct value, not only of the second but also the first order coefficient. We will discuss below the various theoretical values of the first and second order velocity slip coefficients and compare them with the measured values (in Section "First and second order effects").

An analytical approach has recently been proposed [22] for isothermal two dimensional gas flows in micro channels. This approach was based on a conservation equation system (quasi gasdynamic equations (QGD)), using modified closure relations and new expressions of the various fluxes and involving Kn second order terms [23]. In the present work an analytical expression of the streamwise mass flow rate as a function of a pressure and its gradient is obtained under the same assumptions but for a cylindrical geometry:

$$Q_m^T = \frac{\pi D^2 \mu k_\lambda^2}{256 L K n_{out}^2}\left(\mathcal{P}^2 - 1 + 16 A_1 K n_{out}(\mathcal{P}-1) +\right.$$

$$+64\left(A_2+\frac{a}{2k_\lambda^2}\right)\ln \mathcal{P} Kn_{out}^2\Bigg), \qquad (14)$$

where $\mathcal{P}=P_{in}/P_{out}$. It should be noted, that the previous expression is obtained using the second order slip boundary condition (12). The implementation of this condition seems to be more meaningful for the QGD model than for the NS model, because the QGD equations basically involve diffusive terms proportional to the second order of the Knudsen number.

It is possible to consider equation (14) as a generalized expression derived using one of the two approaches: either the Navier-Stokes or the QGD models both with the second order boundary condition (12). In expression (14) coefficient $a=0$ corresponds to the NS equations and $a=1$ to the QGD approach.

It should be noted that the mass flow rate expression given by the QGD model in comparison with NS equations contains one additional term proportional to the second order Knudsen number. This term is phenomenologically different from the corresponding second order term appearing when using the second order velocity boundary condition. In this case, the second order effects are focused on the wall through the slip coefficients. On the contrary, in the additional QGD second order term, the second order effects result from diffusive and collisional effects located in all the flowfield.

Furthermore a non-dimensional mass flow rate may be deduced from relation (14), where a mean Knudsen number denoted Kn_m appears, based on the mean pressure $P_m=0.5(P_{in}+P_{out})$:

$$S=1+8A_1Kn_m+16\left(A_2+\frac{a}{2k_\lambda^2}\right)\frac{\mathcal{P}+1}{\mathcal{P}-1}\ln \mathcal{P} Kn_m^2=$$
$$=Q_m^T/\frac{\pi\Delta P P_m}{8\mu\mathcal{R}TL}\left(\frac{D}{2}\right)^4, \qquad (15)$$

where $\Delta P=P_{in}-P_{out}$. Expression (15) may be rewritten in the more compact form:

$$S=1+A^{theor}Kn_m+B^{theor}Kn_m^2. \qquad (16)$$

The analytical expressions of the mass flow rate (14) – (16) will be used for calculations and comparison with the appropriate measured values.

RESULTS AND DISCUSSION

First comparison of the results

Each experiment was carried out, with a constant pressure ratio $\mathcal{P}$ between the tanks, within the narrow range $4.47-5.02$, centered about $\mathcal{P}=4.75$. The experimental conditions are summarized in Table 4. Nitrogen was used as the working gas. The two methods implemented in the present work were already known, but they were transformed in order to be utilized in new conditions, especially within new pressure ranges. The drop method had previously been applied for outlet pressures higher than $4800Pa$ and so for mass flow rates higher than those considered here except [5], and similarly the pressure rise detection had not been employed with such sensitive gauges. Figure 2 presents the comparison of the mass flow rate measured with the two different techniques for the same outlet Knudsen number range with the analytical solution (14) calculated as a function of the outlet Knudsen number for a fixed pressure ratio $\mathcal{P}=4.7$. The relative experimental error bars vanish when using the logarithmic scale. Thus from Figures 2 we can conclude to a global agreement between the two experimental methods and moreover to their reasonable agreement with the analytical QGD approach.

Figure 3 shows the experimental mass flow rate measured with the two techniques, where the range of the pressure method is extended up to an average Knudsen number $Kn_m\sim 0.3$. The experimental errors shown for the two methods are both of the same order, as seen above ($\pm 4.2\%$ for the drop method and $\pm 4.5\%$ for the pressure method). The experimental results are presented in a non-dimensional form according to the right-hand side of relation (15). Two analytical solutions are also plotted: the analytical solution of NS equations with the first order velocity slip condition, this case corresponds to $A_2=0$, $a=0$ in equation (15), and the analytical solution of the QGD equations

Table 3. Physical constants of N_2 under standard conditions.

Parameter	N_2
Viscosity $(\mu_{ref})(Ns/m^2)\times 10^{-5}$	1.656
Specific gas constant $(\mathcal{R})$(J/kg K)	297.
Viscosity index ω	0.74
k_λ (VHS model)	0.731

Table 4. Experimental pressure range.

Quantity	*Min*	*Max*
Inlet pressure (Pa)	1218.8	121072.
Outlet pressure (Pa)	245.02	24709.
Outlet Knudsen number Kn_{out}	0.0086	0.871
Average Knudsen number Kn_m	0.0029	0.289

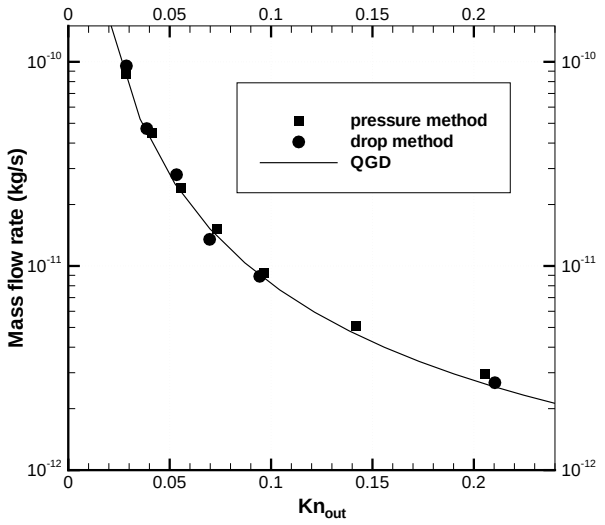

Figure 2. The squares and circles are the experimental measurements. The solid line represents the analytical mass flow rate calculated according to (14) with a fixed pressure ratio $\mathcal{P} = 4.7$.

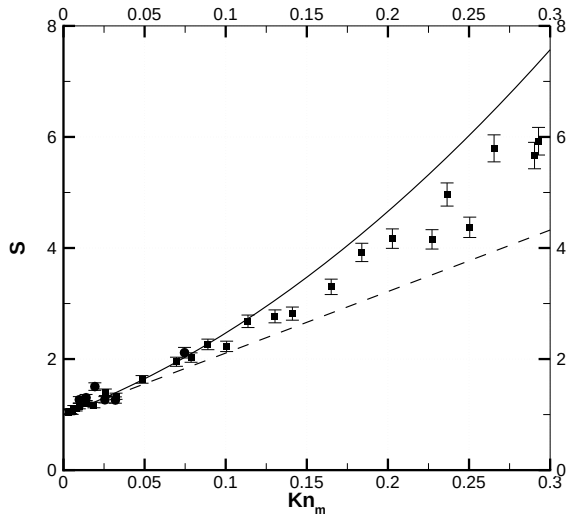

Figure 3. The circles and squares are the experimental measurements. The solid line represents the analytical QGD solution calculated according to equation (15) ($A_2 = 0$, $a = 1$) with fixed pressure ratio $\mathcal{P} = 4.75$. The dashed line is the analytical NS solution (15) with $A_2 = 0$, $a = 0$.

also with the first order velocity slip condition ($A_2 = 0$, $a = 1$ in (15)). The second analytical solution is calculated with two pressure ratio $\mathcal{P} = 4.75$. Figure 3 shows the presence of the second order effects appearing for a mean Knudsen number greater than 0.1. The implementation of the NS equations with the first order boundary condition underestimates the measured mass flow rate while the QGD equations, also with the first order condition, overestimate the measured mass flow rate. This result prompts two comments:

the various theoretical models present differences which can exceed the second order effects;
a second order seems really present anyway and should be further analyzed.

A promising method of measurement

Now, the two methods should be compared with regard to the difficulties encountered during their implementation, and also regarding their possible improvement. The drop method presents the advantage of allowing us direct rough visual control of the flow stationarity. But its implementation brings up various problems:

it is difficult to introduce the oil drop in the calibrated tube without causing a small pressure jump in the second tank;
several drops may form in the calibrated tube, perturbing the velocity and thus the pressure measurements;
one drop may "explode" in the calibrated tube, causing a pressure jump which distorts the measurements. It is to note that the measurement of this jump gives the value $9.59Pa$, which corresponds to the pressure difference upstream-downstream the drop;
it is difficult to precisely estimate the drop-gas interface position in the syringe and to be sure to follow the same point of this interface throughout the experiment.

The pressure method is free of this kind of problems and is very easy to use because all the data are recorded and exploited automatically. Moreover the pressure measurements could be improved: first it is possible to reduce the size of the tanks without calling into question the steady assumption, and thus it would take less time to run the experiments. It is also possible to extend the Kn_m range investigated by diminishing $\mathcal{P}$ (down to about 3) with a reasonable experiment time length (shorter than two hours). Moreover replacing nitrogen with helium as the working gas and considering the respective physical properties of these gases, measurements can be carried out for Kn_m up to 3.5, which corresponds to mass flow rates of about $3 \cdot 10^{-14} kg/s$. The potentials of the second detector theoretically allow P_{out} to be decreased even more, but this is presently limited by a perturbing thermal creep effect induced by the pressure gauges heating [24], [25] which makes a systematic investigation difficult. Nevertheless a perspective is thus opened to obtain experimental mass flow rate data for even higher Knudsen numbers.

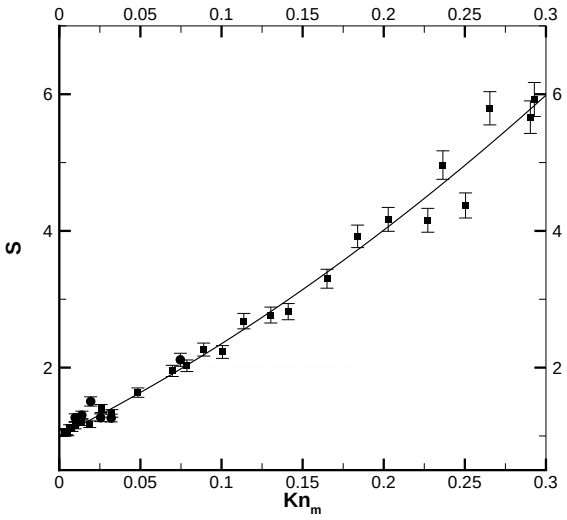

Figure 4. The circles and squares are the experimental measurements. The solid line represents the fitting of the experimental data with the second order polynomial function (17).

Finally, it should be noticed that the difficulties previously pointed out in [7] about the single constant-volume tank disappear under the present experimental conditions: the pressure gauge are sufficiently sensitive and P_{out} sufficiently low to obtain correct isothermal mass flow rate measures, for reasonable time lengths and without significant perturbing effects of temperature variations.

First and second order effects

In addition, the experimental dimensionless mass flow rate data were fitted with a Kn_m second order polynomial form:

$$S_f^{exp} = 1 + A^{exp} Kn_m + B^{exp} Kn_m^2, \tag{17}$$

by using a non-linear least square method, as detailed in [4] with the same working gas, in silicon micro channels with rectangular sections of high width-to-height ratio. Our measures were obtained within narrower pressure ratio range 4.75 ± 0.27 and for Kn_m numbers exclusively relevant to the slip regime. The experimental values obtained for the S_f^{exp} coefficients are: $A^{exp} = 11.92 \pm 0.887$, $B^{exp} = 15.61 \pm 3.746$, where uncertainty is estimated using the asymptotic standard errors. The experimental data of the dimensionless mass flow rate, fitted using the non linear least square method, are presented in Figure 4.

Basing our estimation on two experimental coefficients A^{exp} and B^{exp}, we will estimate the first σ_p and second σ_{2p} velocity slip coefficients in equation (10), according to coefficients A_1 and A_2 in (12).

First order effect. From the comparison of the theoretical (15) and experimental (17) mass flow rate expressions coefficient A_1 may be expressed in the form:

$$A_1 = \frac{\sigma_p}{k_\lambda} = A^{exp}/8. \tag{18}$$

The previous relation gives the experimental estimation of the first velocity slip coefficient $\sigma_p^{exp} = 1.089 \pm 0.081$. This value is close to two theoretical predictions of the slip coefficient: $\sigma_p = 1.012$ given by Kogan [27] and $\sigma_p = 1.016$ given by Cercignani [26] (see Table 5). Both coefficients are obtained from the Boltzmann equation applying the BGK model in the Knudsen layer under the full accommodation assumption of the molecules at the wall.

Then we compared our results with other experimental results. Firstly with those concerning the velocity slip measured by the authors of [12]. They assumed the linear dependence of the mass flow rate on the Knudsen number, which may be justified by the narrow experimental Knudsen number range (below to 0.04) and they obtained the velocity slip coefficient from the flow rate measurements using the linear last square method. The difference between the values of the slip coefficient measured in [12] $\sigma_p = 1.192$ and in the present work may occur because of the implementation of the mass flow rate models involving terms of the different orders in Knudsen number. The use of the second order model allows us to define the velocity slip coefficient more exactly. Moreover it should be noted that the nature of the surfaces for both experiments is not the same: in [12] a packet of glass capillaries with molten walls are used, which may be another reason for the difference observed in the measured values of the velocity slip coefficient. The authors of [12] also derived theoretical results assuming a diffuse molecular scattering at the wall.

Table 5. Experimental and analytical first order velocity slip coefficients.

	σ_p
Kogan [27]	1.012
Cercignani [26]	1.016
Porodnov et al. [12]	1.192 ± 0.021
from present exp.	1.089 ± 0.081

We also derived an experimental value of the accommodation coefficient using the Maxwell diffuse-scattering model. The

use of Maxwell's kernel for the gas-surface interaction gives the following value for the velocity slip coefficient, neglecting the Knudsen layer influence

$$\sigma_p^M = \frac{\sqrt{\pi}}{2}\frac{2-\alpha}{\alpha}, \tag{19}$$

where α is the part of the molecules reflected diffusively. Based on equation (19) and on the measured value of the velocity slip coefficient we can calculate the "experimental" tangential momentum accommodation coefficient using the relation

$$\sigma_p^{exp} = \frac{\sqrt{\pi}}{2}\frac{2-\alpha}{\alpha}, \tag{20}$$

this value of α is given in Table 6 with the the accommodation coefficients obtained by other authors. All measurements were carried out with different experimental techniques and in the channels with different surfaces. It should be noted that in the case of full accommodation, the theoretical coefficient σ_p^M, which does not include the Knudsen layer condition, is equal to 0.886.

Regarding all the results presented about the accommodation coefficient, one can conclude that both descriptions of the molecular reflection from the wall seem convenient: for the physical conditions considered, the fused silica surface may be described as a perfect diffuse surface as well as a quasi diffuse Maxwell surface (according to the accommodation coefficients deduced from the measurements).

Table 6. Experimental tangential momentum accommodation coefficients.

	α
Maurer et al. [4]	0.87 ± 0.03
Colin et al. [6]	0.93
Arkilic et al. [8]	$0.81 - 0.96$
Porodnov et al. [12]	0.925 ± 0.014
from present exp.	0.933 ± 0.037

Second order effect. The value of coefficient B^{exp} confirms that a significant Kn_m second order effect exists. We can calculate "the experimental coefficients" A_2 from the relation:

$$B^{exp} = 16\left(A_2(a) + \frac{a}{2k_\lambda^2}\right)\frac{\mathcal{P}+1}{\mathcal{P}-1}\ln\mathcal{P}. \tag{21}$$

Two different cases are to be considered. From coefficient B^{exp}, we can estimate coefficient A_2 in the second order boundary condition for the QGD model. As mentioned above, the QGD model involves a second order terms in Knudsen number and so requires a second order (also in Knudsen number) boundary condition, more consistently than the NS model. Taking $a = 1$ in equation (21) we obtain $A_2 = -0.597$ or $\sigma_{2p} = -0.318$. Regarding the second order coefficient, a simple meaningful comparison with the velocity slip coefficient obtained in [14] seems very difficult for various reasons. The author of [14] investigated a two-dimensional cartesian symmetry. Therefore, in order to deduce the corresponding second order results in the present cylindrical symmetry, various modelings are required. First, the second order slip coefficient depends on the channel geometry when tangential gradients exist: moreover its geometry dependence itself depends on the molecular interaction modelling [14]. Second, for the QGD model the definition of the mass flux vector [23] is different from the classical NS definition used by the author [14] and the QGD mass flux contains the additional terms proportional to the pressure and velocity gradients. This means that for the QGD model it is necessary to deduce a different form of second order boundary condition taking into account the particular definition of the mass flux and that the negative values of the experimentally deduced A_2 coefficient is not necessarily surprising in the QGD theoretical frames.

Implementation of the second order boundary conditions with the NS equations ($a = 0$ in equation (21)) gives $\sigma_{2p} = 0.181 \pm 0.043$, or $A_2 = 0.339 \pm 0.081$. As mentioned above, the comparison with the coefficients obtained from existing theoretical approaches [14], [15] is very difficult, first of all for geometrical reasons. Both authors considered the rectangular geometries. The value of the second velocity slip coefficient was obtained in [14] from the Boltzmann equation applying the BGK model for the very simple case of Poiseuille flow when the streamwise velocity gradient is equal to zero.This is not the case for the flow studied here. Another theoretical analysis [15] that use the concept of effective mean free path for momentum transfer without implementation of the Boltzmann equation gives a value of the second velocity slip coefficient close to that proposed in [14] and equal to $9\pi/32$ (see Table 7).

Table 7. The second velocity slip coefficients.

	σ_{2p}
Cercignani [14]	0.7667
Deissler [15]	0.883
Maurer et al. [4]	0.204 ± 0.078
from present exp.	0.181 ± 0.043

An experimental study of the second order coefficients was fulfilled in [4]. Besides the difficulty caused by the different geometries respectively used, there were other difficulties arising from the comparison with the measured values [4] are following.

The authors [4] processed a large number of measures obtained for Kn_m increasing up to 0.8 and therefore probably included a transitional regime effect in their results, whereas our experimental correlation was centered on the slip regime. Moreover they calculated results concerning a very wide $\mathcal{P}$ experimental range while our experiments were narrowly focused on $\mathcal{P} = 4.75$.

Finally, the second order coefficient appears very sensitive to the experimental errors, as shown above and as quoted in [4], and these errors in the present work have at least the same order of magnitude as those in [4].

Moreover, as shown in Table 7, the result in [4] agrees with present results.

Conclusion

Two techniques devoted to the measurements of gas mass flow rates in micro channels were implemented for isothermal slip flow regime. The respective errors and uncertainties of both experimental methods were accurately investigated and estimated.

A method based on the measurement of the pressure rise in the constant volume outlet tank was validated by comparing it to the classical drop method and to the analytical results of the QGD and NS continuum approaches. This method was implemented using up-to-date gauges and for low outlet pressures: in these conditions the method is clearly easy to use and suitable for the experimental determination of the micro channel mass flow rates through slip and translational regimes.

The good results obtained in slip regime notably for the accommodation coefficient and our present investigations for higher Knudsen numbers will deepen our understanding of the reflection/accommodation process at the wall and will extend our knowledge on the rarefied flow behavior.

Moreover in slip regime the results confirmed a significant *Kn* second order effect. Nevertheless improvements of the measurement accuracy are still necessary to confirm quantitatively the values obtained for the second order coefficient. A more precise estimation of the channel characteristic dimension is particularly needed. Using such improvements we will generalize pertinent second order velocity slips for various gases.

ACKNOWLEDGMENT

The authors are grateful to the CNRS (Science Research Council) - project number MI2F03-45, the Conseil Régional Provence Alpes Côtes d'Azur and the SERES company for their financial support. They also thank R. Notonier and A. Tonetto from the "Service Commun de Microscopie Electronique".

REFERENCES

[1] HARLEY J, HUANG Y, BAU H AND ZEMEL J (1995) Gas flows in microchannels. J.Fluid Mech 284:257-274

[2] PONG K, HO C, LIU J AND TAI Y 1994 Non-linear pressure distribution in uniform microchannels. In Application of Microfabrication to fluid Mechanics ASME, FED, vol. 197, p 51-56.

[3] ZOHAR Y., LEE S.Y.K., LEE W.Y., JIANG L., TONG P. (2002) Subsonic gas flow in a straight and uniform microchannel, J. Fluid Mech., vol. 472, pp. 125-151.

[4] MAURER J, TABELING P, JOSEPH P AND WILLAIME H (2003) Second-order slip laws in microchannels for helium and nitrogen. Physic of fluid 15:2613-2621

[5] LALONDE P. (2001) Etude expérimentale d'écoulements gazeux dans les microsystèmes à fluides. Ph. D thesis, Institut National des Sciences Appliquées, Toulouse, France.

[6] COLIN, S., LALONDE, P. &CAEN R. (2004) Validation of a second-order slip flow model in rectangular microchannels *Heat Transfer Eng* **25**, No. 3, 23–30.

[7] ARKILIK, E.B., SCHMIDT, M.A. & BREUER, K.S. 1997 Gaseous slip flow in long microchannels, *Journal of Microelectromechanical systems* **6**, No. 2, 167–178.

[8] ARKILIC E, BREUER K AND SCHMIDT M (2001) Mass flow and tangential momentum accommodation in silicon micromachined channels. J.Fluid Mech 437:29-43

[9] YAO, Z., HE, F., DING, Y., SHEN, M. & WANG, X. 2004 Low-speed gas flow subchoking phenomenon in long-constant-area microchannel. In *AIAA Journal*, **42**, N 8, pp. 1517–1521.

[10] JANG J. AND WERELEY S.T. (2004) Pressure distributions of gaseous slip flow in straight and uniform rectangular microchannels, Microfluid Nanofluid, v. 1, pp. 41-51.

[11] W. DONG (1956) University of California Report No.UCRL-3353, 1956.

[12] B.T. PORODNOV, P.E SUETIN, S.F BORISOV AND V.D. AKINSHIN (1974) Experimental investigation of rarefied gas flow in different channels, J. Fluid Mech., vol. 64, pp. 417-437.

[13] S.A TISON (1993) Experimental data and theoretical modeling of gas flows through metal capollary leaks, Vacuum, vol. 44, pp. 1171-1175.

[14] CERCIGNANI, C. (1964) Higher order slip according to the linearized Boltzmann equation, Institute of Engineering Research Report AS-64-19, University of California, Berkeley.

[15] DEISSLER, R. G. (1964) An analysis of second-order slip flow and temperature-jump boundary conditions for rarefied gases *International Journal of Heat and Mass Transfer* **7**, 681–694.

[16] KARNIADAKIS G.E. AND BESKOK A. (2002) Microflows: fundamentals and simulation. Springer, Berlin, Heidelberg, New York.
[17] HADJICONSTANTINOU, N.G. (2003) Comment on Cercignani's second-order slip coefficient *Physics of fluids*, **15**, N 8, 2352–2354.
[18] LANG, H. AND LOYALKA , S.K. (1984) *Physics of Fluid* **27**, 1616.
[19] CHAPMAN, S. & COWLING, T.G. (1970) The mathematical theory of non-uniform gases, third edition, University Press, Cambridge.
[20] BIRD G (1994) Molecular gas dynamics and the direct simulation of gas flows, Oxford University Press, New York.
[21] BARBER, R.W. & EMERSON, D.E. (2005) Challenges in modeling gas-phase flow in microchannels: from slip to transition, Proceeding of ICMM2005, 3rd International Conference on Microchannels and Minichannels, 13-15 June, 2005, Toronto, Canada.
[22] GRAUR I, MÉOLANS J, ZEITOUN D (2005) Analytical and numerical description for isothermal gas flows in microchannels, Microfluidics and Nanofluidics, 1613-4990, Online publication.
[23] ELIZAROVA T AND SHERETOV Y (2001) Theoretical and Numerical Analysis of Quasi-Gasdynamic and Quasi-Hydrodynamic Equation. Comput. Mathem. and Mathem. Phys 41:219-255
[24] JITSCHIN W. AND P. RÖHL (1987) Quantitative study of the thermal transpiration effect in vacuum gauges, J. Vac. Sci. Technol. A, vol 5, No.3, pp. 372-375.
[25] POULTER K. F, M-J. RODGERS, P. J. NASH, T. J. THOMPSON AND M. P. PERKIN (1983) Thermal transpiration correction in capacitance manometers, Vacuum, vol. 33, pp. 311-316.
[26] ALBERTONI S., CERCIGNANI C., GOTUSSO L., (1963) Numerical evaluation of the slip coefficient, Phys. Fluids, **6**, 993-996.
[27] KOGAN M.N. (1969) Rarefied gas dynamics, Plenum Press, New York.